



Transformation of Olfactory Representations in the *Drosophila* Antennal Lobe

Rachel I. Wilson, *et al.*
Science **303**, 366 (2004);
DOI: 10.1126/science.1090782

**The following resources related to this article are available online at
www.sciencemag.org (this information is current as of January 17, 2007):**

Updated information and services, including high-resolution figures, can be found in the online version of this article at:

<http://www.sciencemag.org/cgi/content/full/303/5656/366>

Supporting Online Material can be found at:

<http://www.sciencemag.org/cgi/content/full/1090782/DC1>

This article **cites 27 articles**, 9 of which can be accessed for free:

<http://www.sciencemag.org/cgi/content/full/303/5656/366#otherarticles>

This article has been **cited by** 51 article(s) on the ISI Web of Science.

This article has been **cited by** 13 articles hosted by HighWire Press; see:

<http://www.sciencemag.org/cgi/content/full/303/5656/366#otherarticles>

This article appears in the following **subject collections**:

Neuroscience

<http://www.sciencemag.org/cgi/collection/neuroscience>

Information about obtaining **reprints** of this article or about obtaining **permission to reproduce this article** in whole or in part can be found at:

<http://www.sciencemag.org/help/about/permissions.dtl>

REPORTS

tuates because of seasonal variations in crop performance (16). Production of galactomannan gums in high-yielding commercial crops, such as soybean, should help stabilize their supply and thus price.

Degree of galactosyl substitution on the mannan backbone determines the quality of galactomannan as a gum, e.g., a mannose/galactose ratio of ~4 in locust bean is superior to a ratio of 2 in guar, which is reflected in the significantly higher price of the former (16). The degree of galactosylation of natural galactomannans is believed to be determined by the action of an α -galactosidase later in seed development (27–29). However, an altered pattern of galactosylation of the tobacco seed endosperm galactomannan was obtained by the transgenic expression of the fenugreek α -galactosyltransferase, suggesting that it is possible to affect galactosylation of the naturally occurring galactomannans independent of α -galactosidase (30). Now that all the genes for galactomannan formation have become available (19, 29), it has become possible to reconstitute the galactomannan synthase machinery in other plant species. An attractive scenario is to produce gums of high value, like those of locust bean, as well as novel gums.

References and Notes

- P. M. Ray, T. L. Shninger, M. M. Ray, *Proc. Natl. Acad. Sci. U.S.A.* **64**, 605 (1969).
- P. Kooliman, *Carbohydr. Res.* **20**, 329 (1971).
- A. Bacic, P. J. Harris, B. A. Stone, in *Biochemistry of Plants*, J. Preiss, Ed. (Academic Press, New York, 1988), vol. 14, pp. 297–371.
- S. Cutler, C. Somerville, *Curr. Biol.* **7**, 108 (1997).
- T. A. Richmond, C. R. Somerville, *Plant Physiol.* **124**, 495 (2000).
- S. P. Hazen, C. J. S. Scott, J. D. Walton, *Plant Physiol.* **128**, 336 (2002).
- K. Kudlicka, R. M. Brown Jr., *Plant Physiol.* **115**, 643 (1997).
- K. S. Dhugga, P. M. Ray, *Eur. J. Biochem.* **220**, 943 (1994).
- J. R. Pear, Y. Kawagoe, W. E. Schreckengost, D. P. Delmer, D. M. Stalker, *Proc. Natl. Acad. Sci. U.S.A.* **93**, 12637 (1996).
- T. Arioli et al., *Science* **279**, 717 (1998).
- G. Taylor, W. R. Scheible, S. Cutler, C. R. Somerville, S. R. Turner, *Plant Cell* **11**, 769 (1999).
- I. M. Saxena, R. M. Brown Jr., *Cellulose* **4**, 33 (1997).
- F. Goubet et al., *Plant Physiol.* **131**, 547 (2003).
- B. Favery et al., *Genes Dev.* **15**, 79 (2001).
- X. Wang et al., *Plant Physiol.* **126**, 575 (2001).
- H. Maier, M. Anderson, C. Karl, K. Magnuson, R. L. Whistler, in *Industrial Gums: Polysaccharides and their derivatives*, R. L. Whistler, J. N. BeMiller, Eds. (Academic Press, Inc., London, UK, 1993), pp. 181–226.
- J. S. G. Reid, M. E. Edwards, M. J. Gidley, A. H. Clark, *Biochem. Soc. Trans.* **20**, 23 (1992).
- J. S. G. Reid, M. E. Edwards, M. J. Gidley, A. H. Clark, *Planta* **195**, 489 (1995).
- M. E. Edwards et al., *Plant J.* **19**, 691 (1999).
- R. M. Perrin et al., *Science* **284**, 1976 (1999).
- A. Faik, N. J. Price, N. V. Raikhel, K. Keegstra, *Proc. Natl. Acad. Sci. U.S.A.* **99**, 7797 (2002).
- Materials and methods are available as supporting material on Science Online.
- M. S. Kang et al., *J. Biol. Chem.* **259**, 14966 (1984).
- M. Yoshida, N. Itano, Y. Yamada, K. Kimata, *J. Biol. Chem.* **275**, 497 (2000).
- E. G. T. Wee, D. J. Sherrier, T. A. Prime, P. Dupree, *Plant Cell* **10**, 1759 (1998).
- R. L. Whistler, in *Industrial Gums: Polysaccharides and their derivatives*, R. L. Whistler, J. N. BeMiller, Eds. (Academic Press, San Diego, 1993), pp. 1–19.
- M. Edwards, C. Scott, M. J. Gidley, J. S. G. Reid, *Planta* **187**, 67 (1992).
- C. V. Mujer, D. A. Ramirez, E. M. T. Mendoza, *Phytochemistry* **33**, 893 (1984).
- M. Joersbo, J. Marcussen, J. Brunstedt, *Mol. Breed.* **7**, 211 (2001).
- J. S. G. Reid, M. E. Edwards, C. A. Dickson, C. Scott, M. J. Gidley, *Plant Physiol.* **131**, 1487 (2003).
- We thank K. Kollipara for help with phylogenetic analysis; D. Schmidt and M. Vogt for field support; C. Hainey for cDNA library construction; T. Harp for sugar composition analyses; and the members of the Pioneer Hi-Bred International Discovery Research committee for supporting this work.

Supporting Online Material

www.sciencemag.org/cgi/content/full/303/5656/363/DC1

Materials and Methods

Tables S1 and S2

Figs. S1 to S9

References

28 August 2003; accepted 2 December 2003

Transformation of Olfactory Representations in the *Drosophila* Antennal Lobe

Rachel I. Wilson, Glenn C. Turner, Gilles Laurent*

Molecular genetics has revealed a precise stereotypy in the projection of primary olfactory sensory neurons onto secondary neurons. A major challenge is to understand how this mapping translates into odor responses in these second-order neurons. We investigated this question in *Drosophila* using whole-cell recordings in vivo. We observe that monomolecular odors generally elicit responses in large ensembles of antennal lobe neurons. Comparison of odor-evoked activity from afferents and postsynaptic neurons in the same glomerulus revealed that second-order neurons display broader tuning and more complex responses than their primary afferents. This indicates a major transformation of odor representations, implicating lateral interactions within the antennal lobe.

A major focus of sensory neuroscience is to elucidate the progressive transformations of stimulus representations between layers of neurons in a hierarchy. Olfaction is a structurally shallow modality: In vertebrates, only one layer—the olfactory bulb—separates olfactory sensory neurons (OSNs) from cortex. In *Drosophila* as well, one layer—the antennal lobe—separates OSNs from the mushroom bodies, an association area involved in learning. In terms of its functional architecture, the antennal lobe resembles the olfactory bulb: Each OSN expresses one functional type of odorant receptor, and all or the great majority of OSNs that express the same receptor also target the same glomerulus (1–5). In turn, postsynaptic principal neurons (termed projection neurons, or PNs), like olfactory bulb mitral cells, receive monosynaptic OSN input from a single glomerulus via a singular dendritic tuft (6).

How might this intermediate layer (olfactory bulb or antennal lobe) transform olfactory representations? One hypothesis is that the tuning curves of each glomerular channel are sharpened by lateral inhibition (7, 8). Another idea is that synaptic interactions in this layer

distribute activity across the network and impose odor-specific slow temporal patterns (9, 10). Finally, no transformation at all may occur between OSNs and higher association areas (11, 12). We addressed this issue using whole-cell patch-clamp recordings in the *Drosophila* antennal lobe, which has only about 40 glomeruli with stereotyped positions, meaning that each PN can be matched to its input glomerulus (13). Because genetically labeled *Drosophila* OSNs are accessible to single-unit recording (5, 14–16), we could directly compare the tuning of OSNs and PNs corresponding to the same glomerulus.

Recordings were obtained from 43 PNs; 40 of these were identified morphologically from dye fills (Fig. 1A), and 3 were identified genetically in flies in which only PNs express green fluorescent protein (GFP) (*GHI46-Gal4, UAS-CD8-GFP*) (17). These PNs collectively sampled from at least 20 different glomeruli. During recordings, flies exhibited spontaneous movements of the legs and proboscis, abundant spontaneous neural activity, and stable odor responses (18).

Even in the absence of stimuli, PNs typically received a continuous barrage of excitatory postsynaptic potentials (EPSPs), and fired spontaneously (mean rate = 4 ± 0.7 Hz). In contrast to action potentials in local neurons, which were always > 40 mV in am-

Division of Biology, 139-74, California Institute of Technology, Pasadena, CA 91125, USA.

*To whom correspondence should be addressed. E-mail: laurentg@caltech.edu.

plitude, spikes recorded in PN somata were <10mV (Fig. 1B). Spontaneous EPSPs in PNs were blocked by a nicotinic acetylcholine receptor antagonist, and spikes were abolished by tetrodotoxin (fig. S1).

We used a large and chemically diverse stimulus set (33 odors) to probe the antennal lobe representation of olfactory space. All odors were used at 1000-fold dilutions (18), well within the dynamic range of *Drosophila* OSNs (15, 16). Each odor activated different PN ensembles (Fig. 1C), consistent with imaging data (11, 12, 19). On average, each odor elicited excitatory responses in $69 \pm 3\%$ of PNs (averaged across 33 odors, threshold 2 SDs above each PN's baseline firing rate). Fig. 1D shows the distribution of odors according to the percentage of PNs that they excited. For example, cyclohexanone excited 85% of PNs tested, so this odor is one of the five odors in the ninth bin of the histogram. This distribution shows that most odors elicited responses from a large PN ensemble. Excitatory responses differed in magnitude across PNs, but each ensemble typically included many intense responses, and on average a single odor triggered responses >50 Hz above baseline in $52 \pm 3\%$ of PNs (Fig. 1E). Many responses (38%) had both excitatory and inhibitory epochs (e.g., in Fig. 1C, benzaldehyde: glomeruli VC1 and D). Odor patterns were distinctive in the identity of both the PNs that were activated and those that were inhibited, as well as in their temporal patterning (Fig. 1C).

PNs arborizing in the same glomerulus, recorded in different flies, responded similarly to odors (Fig. 1F). This result is consistent with the stereotyped map of OSN inputs to the antennal lobe (3, 4) and with the notion that OSN input is a major determinant of PN tuning. Responses across flies were similar not just in intensity but also in temporal pattern, implying that odors elicit stereotyped dynamics in the antennal lobe network (20).

Although responses of PNs within a glomerulus were similar, responses varied greatly across glomeruli. There was no typical response pattern or tuning width. Some PNs were excited by almost all odors tested (Fig. 2, A, C, and E), whereas others were inhibited by all odors (Fig. 2B). Yet others showed marked preferences, although a PN's preferred odors were usually not restricted to a small or easily classified chemical group (Fig. 2, D and F). On average, $60 \pm 6\%$ of odors elicited an excitatory response in a given PN (averaged across cells, restricted to the 37 PNs exposed to at least five odors). However, the histogram of PN response probability is skewed toward low and high response probabilities (Fig. 2G).

At the low end of the distribution, some PNs are specialists (e.g., Fig. 2B), and one-fifth (8/37) were excited by none of the odors tested. These cells may be tuned to odors not included in our stimulus set, including perhaps compounds of special behavioral relevance. Interestingly, five of these specialist cells innervated a lateral-anterior glomerulus (VA1d, VA1lm, VA5, and VA6). One lateral-anterior glomerulus, VA1, is sexually dimorphic and is innervated by OSNs from trichoid antennal sensilla, some of which are selective for a putative *Drosophila* pheromone (4, 14, 21, 22).

At the other end of the distribution, many PNs are generalists (Fig. 2G). This

broad tuning may be surprising, given that OSNs have been shown to be more narrowly tuned under stimulus conditions very similar to ours (15, 16). We hypothesized, therefore, that some PNs might be more broadly tuned than their monosynaptic OSN afferents. We thus compared OSNs and PNs corresponding to a single glomerulus, DM2. This glomerulus is targeted by OSNs expressing the olfactory receptor gene *Or22a* (4, 5). We used a fly line in which the *Or22a* promoter drives GFP expression (*Or22a-Gal4, UAS-CD8-GFP*) to identify sensilla on the antenna containing *Or22a*⁺ OSNs. This sensillum type contains two OSNs, and recordings from GFP⁺

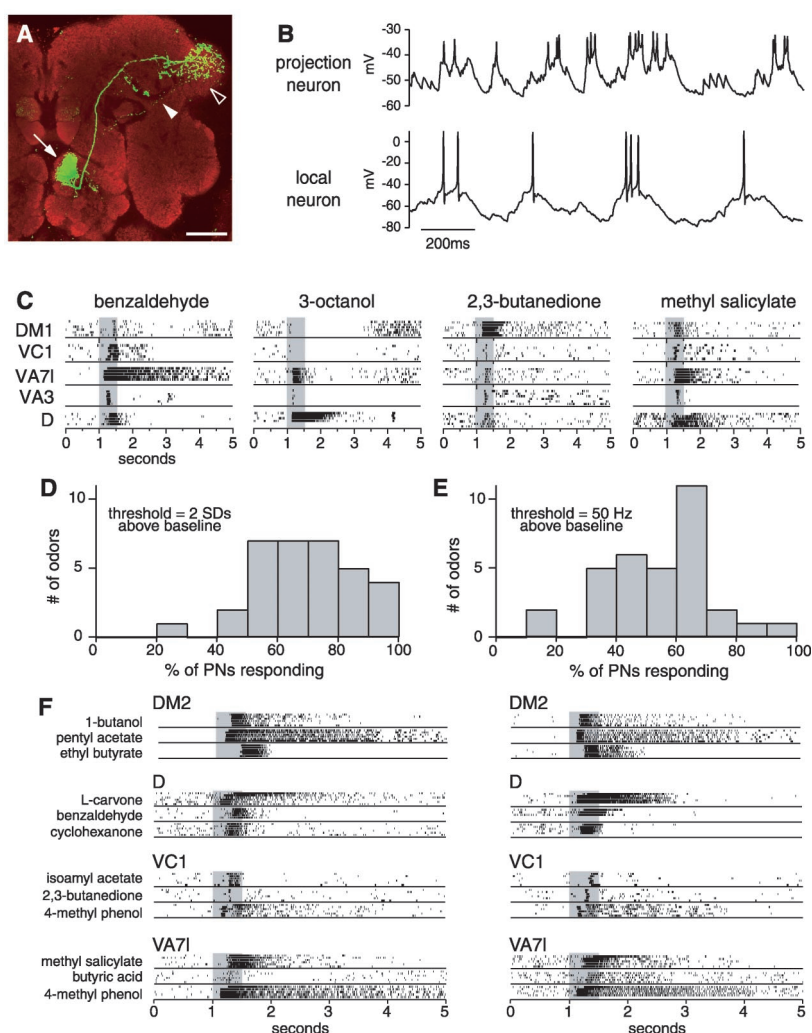


Fig. 1. Odors evoke consistent glomerulus-specific patterns of PN activity. (A) Projection of a confocal stack showing the morphology of a biocytin-filled PN (green) labeled with fluorescent-conjugated streptavidin. An antibody to *Drosophila* neuropil (nc82, red) defines the contours of the brain. Arrow, antennal lobe glomerulus; filled arrowhead, mushroom body calyx; open arrowhead, lateral protocerebrum. Scale bar, 40 μ m. (B) Spontaneous activity recorded in the soma of a PN (upper trace) and LN (lower trace). (C) Rasters of odor responses; the glomerulus containing the dendrites of each recorded PN is indicated along the left edge of the panel; same glomeruli for all four odors. Gray bars, odor. (D) Histogram showing the distribution of the 33 test odors on the basis of the percentage of PNs they excited. The firing-rate threshold for an excitatory response was 2 SDs above the baseline. (E) Threshold, 50 Hz above baseline. (F) Rasters show odor responses of PNs innervating the same glomerulus in different flies (left and right columns).

REPORTS

sensilla in these flies (Fig. 3A) show two spike sizes. The larger spikes (green symbols in Fig. 3, A and C) are known to arise from the *Or22a*⁺ OSN (5). In parallel experiments with flies of the same genotype, we recorded from PNs innervating glomerulus DM2, identified post hoc by intracellular dye labeling. Fig. 3B shows dendrites of the filled PN (red) converging unilaterally on the same glomerulus as the OSN axons (green). The glomerular identity of all five DM2 PNs was confirmed by overlap of GFP⁺ axons and dye-filled dendrites.

A comparison of PN and OSN rasters (Fig. 3, C and D) revealed that a DM2 PN could be strongly excited by an odor that was a poor stimulus for its presynaptic OSNs. Odors that excited DM2 PNs could elicit no detectable response (Fig. 3C) or a weak response with long latency (Fig. 3D) in *Or22a*⁺ OSNs. The other OSN in this sensillum does not express *Or22a* and is thought to target a different glomerulus (5).

This OSN served as a positive control in these examples (Fig. 3, A, C, and D, blue symbols), demonstrating that these odors, although ineffective in activating the *Or22a*⁺ OSN, were nevertheless good stimuli for other OSNs.

Fig. 3E shows superimposed average peristimulus-time histograms (PSTHs) of *Or22a*⁺ OSNs and DM2 PNs for 12 odors, arranged from strongest to weakest OSN response ($n = 43$ sensilla in 17 flies; $n = 5$ PNs in 5 flies). Not only do the PNs and OSNs have different odor preferences, but the shape of the PN PSTH often differed from the shape of the OSN PSTH (Fig. 3E, fig. S2). It is therefore likely that PN responses are shaped by inputs other than the OSNs targeting their glomerulus (23). These may include recurrent excitatory connections within the antennal lobe, analogous to lateral excitation across glomeruli in the mammalian olfactory bulb (24). Relief from tonic inhibition could also ac-

count for excitatory PN responses not predicted from their monosynaptic OSN inputs.

We constructed mean tuning curves for these OSNs and PNs at different epochs in the response (Fig. 3F). PNs were more broadly tuned than OSNs, and whereas OSN tuning curves were skewed toward high and low response strengths, PN tuning curves were flatter, with more intermediate responses. We quantified this difference using a measure of tuning curve sharpness (*S*, lifetime sparseness) (25, 26). By this measure, the PN tuning curves showed consistently less selectivity than the OSN tuning curves. PNs summate inputs from many convergent OSNs, and a flatter tuning curve could be achieved in principle by summation, together with a ceiling on PN firing rates that would truncate the top of their tuning curve. However, because the rank of PN odor preferences was different from OSN preferences (Fig. 3F), these two mechanisms alone cannot account for the differences between the tuning curves. In addition, whereas there was a modest significant correlation between the OSN and PN tuning curves during the first 100 ms of the response ($r^2 = 0.17$, $P < 0.05$, Pearson's test comparing mean firing rates), during the next 100 ms the OSNs and PNs were completely decorrelated ($r^2 = 0.01$, $P = 0.58$). This comparison implies that PN odor responses arise from a nonlinear transformation of OSN inputs and that this transformation evolves over time, consistent with a role for dynamic synaptic interactions within the antennal lobe.

By analogy with the center-surround antagonism of retinal ganglion cells, it has been suggested that lateral inhibition narrows the tuning of mitral cells and PNs compared with their OSN inputs (7, 8). We observed just the opposite for glomerulus DM2: PNs were more broadly tuned than OSNs, also consistent with the high response probability of most PNs (Fig. 2G). Nevertheless, inhibition is clearly a component of the ensemble odor representation: We observed epochs when PN firing was suppressed below baseline rates in 64% of all odor responses (averaged across all trials with a spontaneous firing rate of at least 0.4 Hz) (Figs. 1 and 2). This prolonged inhibition did not always follow a burst (e.g., Fig. 2B) and is thus unlikely to arise from intrinsic PN conductances. Furthermore, PN PSTHs generally fell off more sharply than the corresponding OSN PSTHs (Fig. 3E), suggesting an inhibition of PN odor responses. Therefore, we investigated mechanisms by which odors could recruit inhibitory synapses in the antennal lobe.

Most local neurons (LNs) in the antennal lobe release the inhibitory neurotransmitter γ -aminobutyric acid (GABA) (6). Intracellu-

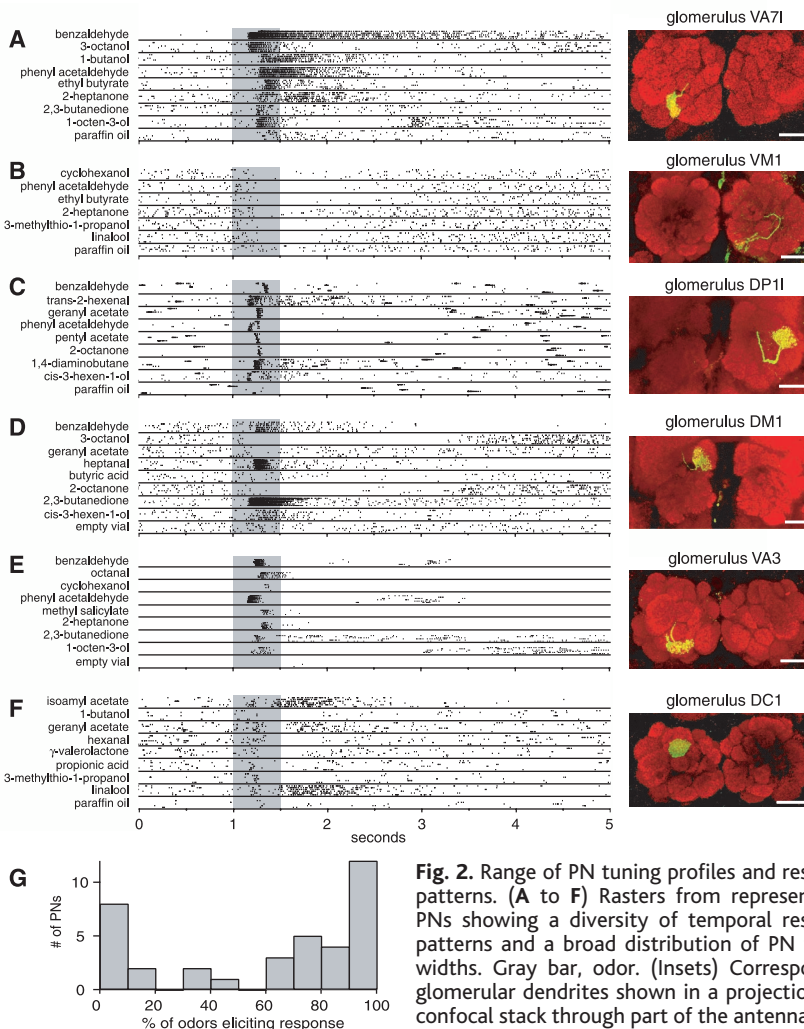


Fig. 2. Range of PN tuning profiles and response patterns. (A to F) Rasters from representative PNs showing a diversity of temporal response patterns and a broad distribution of PN tuning widths. Gray bar, odor. (Insets) Corresponding glomerular dendrites shown in a projection of a confocal stack through part of the antennal lobe. Green signal near the midline in some images

reflects material in the esophagus with streptavidin affinity. Scale bars, 20 μ m. (G) Histogram showing the distribution of PNs on the basis of tuning width. Responses defined as firing rates $>2SDs$ of baseline.

lar dye fills showed that LNs ramified throughout the ipsilateral lobe (Fig. 4, A and B), and varicosities were observed in most or all glomeruli ($n = 5$ fills). Consistent with this morphology, LNs were very broadly tuned to odors, typically responding to every stimulus with a burst of action potentials ($n = 11$) (Fig. 4, C to E).

It has been shown previously that *Drosophila* PNs release neurotransmitter within the antennal lobe (11). We asked, therefore, whether synaptic excitation from PNs might contribute to LN odor responses. We observed that in a simultaneous recording from a PN and an LN, each action potential in the PN evoked by depolarizing current injection triggered an EPSP in the LN with a consistent short latency, implying a monosynaptic connection (Fig. 4, F and G) (27). This result shows that at least some antennal lobe neurons receive excitation from PNs.

LN odor responses were always confined to a brief period (Fig. 4, C and D) that does not match the long inhibitory epochs in many PN odor responses (Figs. 1 and 2). This suggests that fast inhibition by GABA_A-type receptors cannot account for the prolonged inhibition of PNs. We thus examined the effect of a GABA_A antagonist on PN odor responses. Picrotoxin did not eliminate the prolonged suppression of PNs (Fig. 4H). However, blocking fast inhibition did increase PN spiking rates during the first 400 ms of the odor response, as predicted by the period of LN activity (Fig. 4, H and I). Picrotoxin could also uncover latent PN responses (e.g., Fig. 4H, 3-octanol). Thus, even early phases of odor-evoked activity in PNs reflect a balance of excitation and inhibition in the antennal lobe network. The later, prolonged periods of PN inhibition may be attributable to metabotropic receptors. These epochs were associated with a decrease in EPSP frequency (Fig. 4, J and K), suggestive of presynaptic inhibition. Presynaptic inhibition through GABA_B receptors has been described at OSN–mitral cell synapses in the olfactory bulb (28, 29).

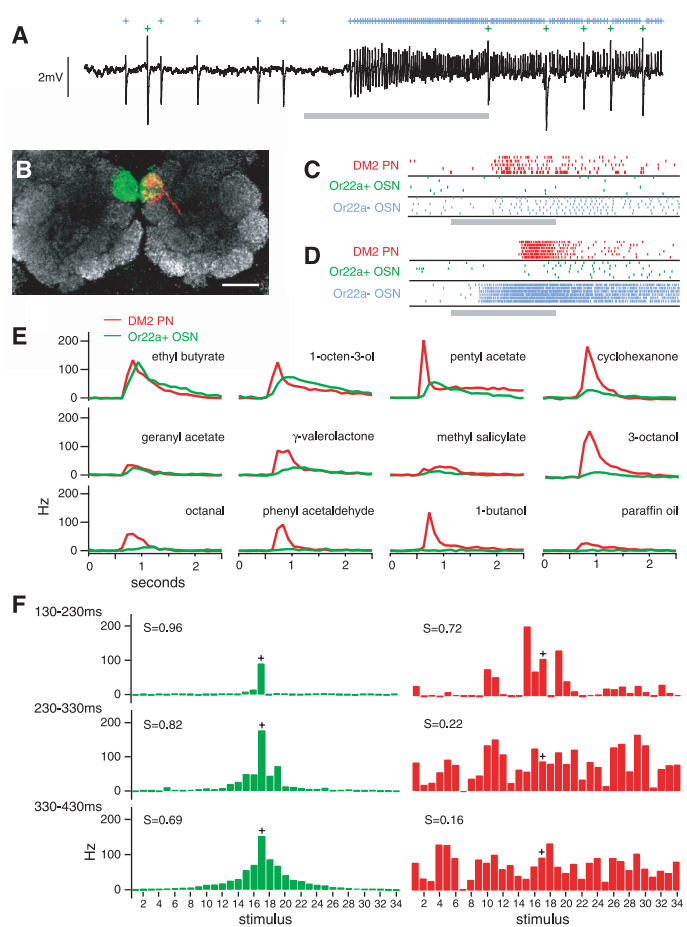
Odor-evoked PN activity in *Drosophila* has been visualized by using genetically encoded reporters of calcium and vesicular exocytosis (11, 12). These studies concluded that PNs mirror almost perfectly the activity of their monosynaptic OSN inputs. There are several possible explanations for why these studies have come to conclusions different from ours. First, the relation between the signals from these reporters and spiking activity has not been characterized. Specifically, these reporters might only signal high spiking rates. Alternatively, because insect nicotinic acetylcholine receptors are highly permeable to calcium, a sensor that directly or indirectly reflects intracellular calcium may be more correlated with synaptic excita-

tion than with spike-mediated output (30, 31). Second, the fluorescence of a genetically encoded sensor depends on the strength of the promoter driving its expression and cannot be quantitatively compared across different Gal4-driver lines without appropriate calibration (32).

Our electrophysiological results yield a picture of the antennal lobe as actively shaping responses to odors. We describe a diverse set of PN tuning properties: “Specialists” may reflect an evolutionary need for high discrimination acuity among odors with special behavioral relevance, such as pheromones (33). By contrast, “generalists” participate in many odor-evoked ensembles. Specialists and generalists have previously been noted among OSNs (34). By directly comparing presynaptic and postsynaptic tuning curves corresponding to the same glomerulus, we show that generalist PNs can be even more broadly tuned than their monosynaptic OSN inputs. This

is likely to be true for other glomeruli as well, because studies using odors and concentrations similar to ours report that a large fraction of OSNs are more narrowly tuned than most of our “generalist” PNs (15, 16). Thus, many PNs appear to integrate information across OSN channels, despite their uniglomerular dendritic fields, reflecting lateral interactions within the antennal lobe. One possible advantage of this arrangement is to facilitate decoding of the representations of a large number of noisy stimuli by separating odor clusters in stimulus space (fig. S3). Because *Drosophila* affords selective genetic control over neural circuits, the importance of these transformations should be testable by behavioral experiments. Thus, in bridging the longstanding gap in *Drosophila* between molecules and behavior, electrophysiological approaches complement the power of this model organism to reveal relations between genes, perception, and experience.

Fig. 3. Comparison of presynaptic and postsynaptic odor-evoked spikes in glomerulus DM2. (A) Extracellular recording of two OSNs in the same antennal sensillum. The larger spikes (green symbols) arise from the GFP⁺ OSN expressing *Or22a*, which projects to DM2 (5). Gray bar, 500 ms puff of 2-octanone. (B) A confocal slice through the antennal lobe (1 μ m) of an *Or22a-Gal4, UAS-CD8-GFP* fly. Biotin/streptavidin (red) labels the dendrites of the single PN that was filled. GFP (green) labels afferent terminals converging bilaterally on glomerulus DM2. Scale bar, 20 μ m. (C and D) Rasters from a DM2 PN (red), *Or22a*-positive OSN (green), and *Or22a*-negative OSN (blue) stimulated with 1-heptanol (C) or 2-octanone (D). Gray bar, 500-ms odor puff. (E) Mean PSTHs for *Or22a*⁺ OSNs (green) and DM2 PNs (red). All PSTHs represent responses relative to the spontaneous firing rate during that trial’s baseline period. All panels use the same axes. Odor from 0.5 to 1.0 sec. (F) Tuning curves at different time bins after stimulus onset. Mean firing rate (in that bin) is plotted against stimulus identity, with stimuli arranged along the x axis to produce the maximally smooth tuning curve at 330 to 430 ms for the OSNs. Each value in the tuning curve represents the mean of three to five cells. All panels use the same axes. Sparseness (S) of the distribution is indicated on each panel (25). Symbols (+) mark isoamyl acetate. Stimuli 2 and 3 are empty vial and paraffin oil, respectively. See methods (78) for the 32 odor stimuli.



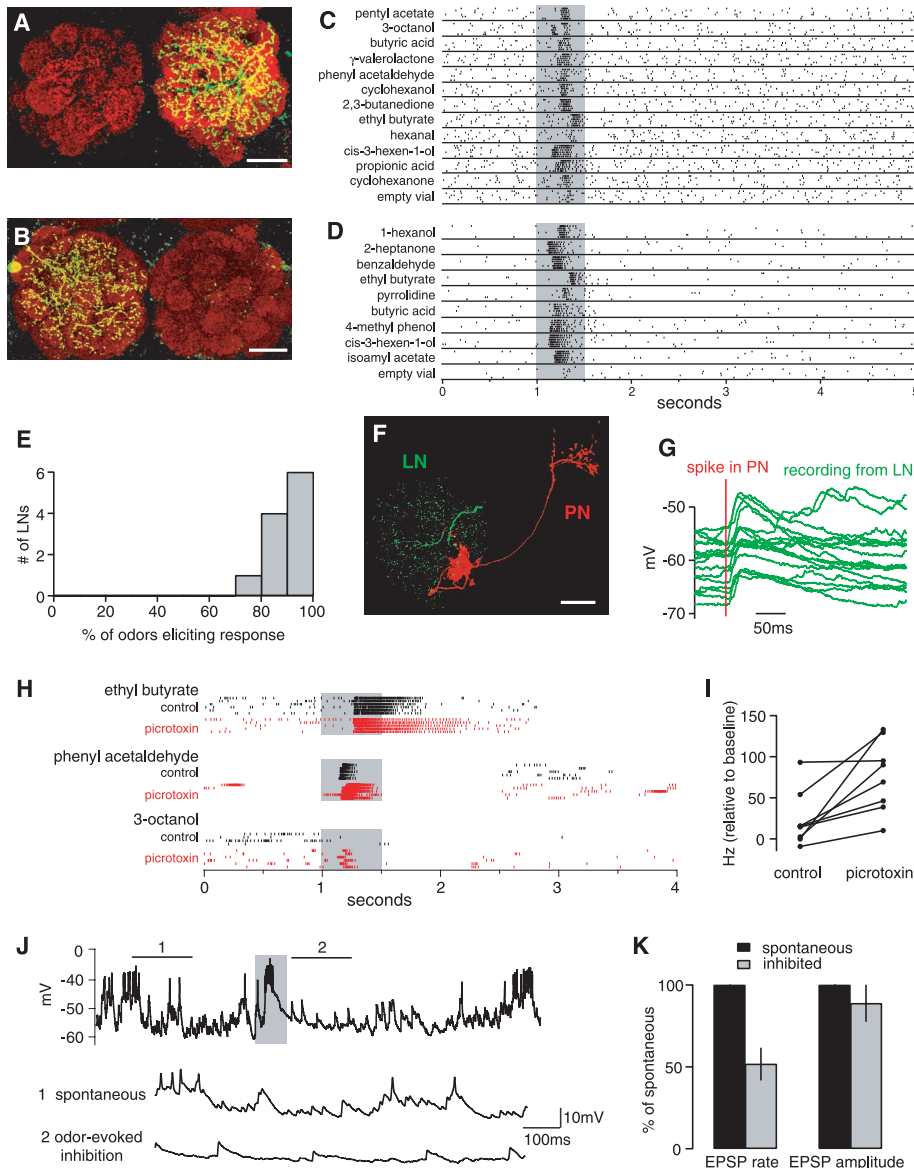


Fig. 4. Inhibitory circuits in the antennal lobe. (A and B) LN morphology in projections of confocal stacks. Scale bars, 20 μ m. (C and D) Rasters show typical odor-evoked activity in two LNs. Gray bars, odor. (E) Histogram showing the distribution of LNs ($n = 11$) on the basis of tuning width, analogous to Fig. 2G for PNs. LNs were identified on the basis of their morphology after dye filling ($n = 5$) or as GFP⁺ antennal-lobe neurons in *GH298-Gal4, UAS-CDB-GFP* flies ($n = 6$). (F) Simultaneous recording of dye-filled LN (green) and PN (red). Scale bar, 20 μ m. (G) Segments of the LN recording are aligned to the time of presynaptic PN depolarization, showing an evoked unitary EPSP in the LN. (H) Rasters displaying odor responses of the same PN before and after addition of picROTOXIN (250 μ M). Gray bars, odor. (I) PicROTOXIN increases the mean spiking rate in PNs during the first 400 ms of the odor response ($P < 0.05$, paired t test; $n = 8$ odors, 3 PNs). (J) Recording from a PN. Enlarged portions below display (1) spontaneous activity and (2) odor-evoked inhibition. Gray bar, odor. (K) EPSP frequency (normalized to spontaneous rate) decreases during epochs of prolonged inhibition after odor onset ($P < 0.01$, paired t test; $n = 5$ cells). EPSP amplitude is not significantly changed ($P = 0.38$, paired t test).

References and Notes

1. K. Scott *et al.*, *Cell* **104**, 661 (2001).
2. L. B. Vosshall, H. Amrein, P. S. Morozov, A. Rzhetsky, R. Axel, *Cell* **96**, 725 (1999).
3. Q. Gao, B. Yuan, A. Chess, *Nature Neurosci.* **3**, 780 (2000).
4. L. B. Vosshall, A. M. Wong, R. Axel, *Cell* **102**, 147 (2000).
5. A. A. Dobritsa, W. van der Goes van Naters, C. G. Warr, R. A. Steinbrecht, J. R. Carlson, *Neuron* **37**, 827 (2003).
6. R. F. Stocker, *Cell Tissue Res.* **275**, 3 (1994).
7. M. Yokoi, K. Mori, S. Nakanishi, *Proc. Natl. Acad. Sci. U.S.A.* **92**, 3371 (1995).

8. S. Sachse, C. G. Galizia, *J. Neurophysiol.* **87**, 1106 (2002).
9. G. Laurent, M. Wehr, H. Davidowitz, *J. Neurosci.* **16**, 3837 (1996).
10. R. W. Friedrich, G. Laurent, *Science* **291**, 889 (2001).
11. M. Ng *et al.*, *Neuron* **36**, 463 (2002).
12. J. W. Wang, A. M. Wong, J. Flores, L. B. Vosshall, R. Axel, *Cell* **112**, 271 (2003).
13. P. P. Laissue *et al.*, *J. Comp. Neurol.* **405**, 543 (1999).
14. P. Clyne, A. Grant, R. O'Connell, J. R. Carlson, *Invert. Neurosci.* **3**, 127 (1997).

15. M. de Bruyne, K. Foster, J. R. Carlson, *Neuron* **30**, 537 (2001).
16. M. de Bruyne, P. J. Clyne, J. R. Carlson, *J. Neurosci.* **19**, 4520 (1999).
17. R. F. Stocker, G. Heimbeck, N. Gendre, J. S. de Belle, *J. Neurobiol.* **32**, 443 (1997).
18. Materials and methods are available as supporting material on Science Online.
19. S. Korsching, *Curr. Opin. Neurobiol.* **12**, 387 (2002).
20. Subtle differences across PNs in the same glomerulus may reflect true differences among the three to five PNs innervating each glomerulus, differences among individual flies, or variability across preparations.
21. R. F. Stocker, R. N. Singh, M. Schorderer, O. Siddiqi, *Cell Tissue Res.* **232**, 237 (1983).
22. Y. Kondoh, K. Kaneshiro, K. Kimura, D. Yamamoto, *Proc. R. Soc. London Ser. B* **270**, 1005 (2003).
23. We noted a weak PN response to the small mechanical component of the stimulus (which was generally the same as the response to paraffin oil, bottom row, Fig. 3E) to which the OSNs did not respond. This result suggests that PNs may also receive indirect input from mechanosensory antennal afferents, which terminate immediately posterior to the olfactory glomeruli.
24. J. S. Isaacson, *Neuron* **23**, 377 (1999).
25. B. Willmore, D. J. Tolhurst, *Network Comput. Neural Syst.* **12**, 255 (2001).
26. Lifetime sparseness, S , ranges from 0 (for a neuron that responds equally to all stimuli) to 1 (for a neuron that is excited by one stimulus and shows zero response to all others).
27. One connection was detected in nine paired recordings. No inhibitory connections were detected in these pairs, which may reflect a low LN to PN connectivity or a unitary conductance that is too small or electrotonically distant to be detected in the soma. Also, we cannot exclude the possibility that the effect of picROTOXIN on PN odor responses may be indirect, reflecting disinhibition of lateral excitatory inputs.
28. M. Wachowiak, L. B. Cohen, *J. Neurosci.* **19**, 8808 (1999).
29. V. Aroniadou-Anderjaska, F. M. Zhou, C. A. Priest, M. Ennis, M. T. Shipley, *J. Neurophysiol.* **84**, 1194 (2000).
30. F. Goldberg, B. Grunewald, H. Rosenboom, R. Menzel, *J. Physiol. (Lond.)* **514**, 759 (1999).
31. T. G. Oertner, T. M. Brotz, A. Borst, *J. Neurophysiol.* **85**, 439 (2001).
32. One study has described a strong correlation between OSN- and PN-derived signals in the same glomerulus, but only when the OSN map was visualized using a higher odor concentration than that used to visualize the PN map (12). The necessity for this higher stimulus concentration was attributed to a weak OSN Gal4-driver but may also reflect a genuine difference between OSN and PN odor responses, as we show here.
33. T. A. Christensen, J. G. Hildebrand, *Curr. Opin. Neurobiol.* **12**, 393 (2002).
34. J. G. Hildebrand, G. M. Shepherd, *Annu. Rev. Neurosci.* **20**, 595 (1997).
35. We thank L. Luo, L. Vosshall, R. Stocker, and S. Benzer for fly lines, E. Buchner and A. Hofbauer for nc82 antibody, D. Darcy and M. Dickinson of the Caltech Biological Imaging center for technical assistance, and J. R. Carlson and W. van der Goes van Naters for sharing methods and flies. We thank M. Stopfer, W. D. Tracey, and members of the Laurent lab for helpful discussions. This work was supported by the Helen Hay Whitney Foundation (R.I.W.), the Jane Coffin Childs Foundation (G.C.T.), the McKnight and Keck Foundations, the National Science Foundation, and the National Institute on Deafness and Other Communication Disorders (G.L.).

Supporting Online Material
www.sciencemag.org/cgi/content/full/1090782/DC1
 Materials and Methods
 Figs. S1 to S3
 References

25 August 2003; accepted 21 November 2003
 Published online 18 December 2003;
 10.1126/science.1090782
 Include this information when citing this paper.